Available online at www.sciencedirect.com
ScienceDirect
Nuclear Physics A 00 (2017) 1–4
Nuclear Physics A
www.elsevier.com/locate/procedia

arXiv:1704.05329v1 [nucl-ex] 18 Apr 2017

Net-baryon fluctuations measured with ALICE at the CERN LHC

Anar Rustamov (for the ALICE Collaboration)[a,b,c,d]

[a]*Azerbaijan National Academy of Sciences, Institute of Physics, Baku, Azerbaijan*
[b]*Physikalisches Institut, Universität Heidelberg, Heidelberg, Germany*
[c]*Extreme Matter Institute EMMI, GSI, Darmstadt, Germany*
[d]*National Nuclear Research Center, Baku, Azerbaijan*

Abstract

First experimental results are presented on event-by-event net-proton fluctuation measurements in Pb- Pb collisions at $\sqrt{s_{NN}}$ = 2.76 TeV, recorded by the ALICE detector at the CERN LHC. The ALICE detector is well suited for such studies due to its excellent particle identification capabilities and large acceptance, which is crucial for fluctuation analysis. The studies are focussed on second order cumulants, but the analysis technique used is more general and will be applied, in the near future, also to higher order cumulants.

Keywords: Quark-gluon plasma, Fluctuations, Conservation laws

1. Introduction

Phase transitions in strongly interacting systems can be addressed by investigating the response of the system to external perturbations via fluctuations of conserved charges. In particular, one can look for critical fluctuations at vanishing baryon chemical potential as reported in [1, 2]. However, fluctuations of conserved charges are predicted in the Grand Canonical Ensemble (GCE) formulation of thermodynamics [3]. In this formulation, the net-baryon number is not conserved in each micro-state, hence it fluctuates. In order to compare theoretical calculations within GCE, such as the Hadron Resonance Gas (HRG) model [4] and Lattice QCD (LQCD) [1], to experimental results, the requirements of GCE have to be achieved in experiments. This is typically done by analysing the experimental data in a finite acceptance by imposing cuts on rapidity and/or transverse momentum of detected particles. However, if the selected acceptance window is too small, the possible dynamical correlations we are after will also be strongly reduced [5] and consequently, net-baryons will be distributed according to the difference of two independent Poisson distributions [6]. We remind that for the Poisson distribution, all its cumulants are equal to its mean. The probability distribution of the difference X_1 - X_2 of two random variables, each generated from statistically independent Poisson distributions, is called the Skellam distribution. According to the additivity of cumulants, the cumulants of the Skellam distribution will then be $\kappa_n(Skellam) = \langle X_1 \rangle + (-1)^n \langle X_2 \rangle$, where $\langle X_1 \rangle$ and $\langle X_2 \rangle$ are mean values of X_1 and X_2 respectively.

On the other hand, the increase of the acceptance will enlarge significance of correlations due to baryon number conservation. In order to be more sensitive to dynamical fluctuations, the better approach is to

study the fluctuation of conserved charges in a larger acceptance and subtract the correlation part caused by the global conservation laws. This is actually the appropriate way to address the fluctuation physics when both, trivial and dynamical fluctuations are close to Poisson probability distributions. To proceed further we provide the necessary definitions. The first and second cumulants of net-baryon $\Delta n_B = n_B - n_{\bar{B}}$ distribution is defined as:

$$\kappa_1(\Delta n_B) = \langle \Delta n_B \rangle \,, \tag{1}$$

$$\kappa_2(\Delta n_B) = \left\langle \Delta n_B^2 \right\rangle - \langle \Delta n_B \rangle^2 \,. \tag{2}$$

The second cumulant can be represented as a sum of corresponding cumulants for single baryons plus the correlation term for joint probability distributions of baryons and antibaryons

$$\kappa_2(\Delta n_B) = \kappa_2(n_B) + \kappa_2(n_{\bar{B}}) - 2\left(\langle n_B n_{\bar{B}} \rangle - \langle n_B \rangle \langle n_{\bar{B}} \rangle\right), \tag{3}$$

Eq. 3 shows that, in the case of missing correlations between baryons and antibaryons, the second cumulant of net-baryons is exactly equal to the sum of the corresponding second cumulants for baryons and antibaryons.

A correlation can emerge, in addition to that originating from critical fluctuations, from conservation laws. If the experimental acceptance is large enough the correlation term in Eq. 3 acquires a finite value. Hence we expect that the second cumulant of net-baryons becomes smaller than the sum of baryons and antibaryons.

We note that in this work net-protons are used as a proxy for net-baryons, which is justified at LHC energies [7].

2. The experimental data and analysis method

The results presented are obtained by analysing about 13 million minimum-bias Pb-Pb events at $\sqrt{s_{NN}} = 2.76$ TeV recorded by the ALICE detector [8] in the year 2010. The detectors used are the Time Projection Chamber (TPC) for tracking and particle identification and the Inner Tracking System (ITS) for precise vertex determination. Both devices are located in the central barrel of the experiment and operate inside a large solenoidal magnet with $B = 0.5$ T. Two forward scintillator hodoscopes V0 are located on either side of the interaction point and cover pseudorapidity intervals $2.8 < \eta < 5.1$ and $-3.7 < \eta < -1.7$. The minimum-bias trigger condition is defined by the coincidence of hits in both V0 detectors. The event centrality is selected based on the signal amplitudes in the V0 detectors. The phase space coverage is restricted to $0.6 < p[\mathrm{GeV/c}] < 1.5$, and $|\eta| < 0.8$. Moreover, differential analysis is provided as function of $\Delta\eta$. High precision particle identification in a wide momentum range is achieved by correlating the measured particle momentum with its specific energy loss dE/dx in the gas volume of TPC. The cumulants of net-protons are reconstructed using a novel approach, the Identity Method, which overcomes incomplete particle identification event-by-event, caused by the overlapping dE/dx distributions [9, 10, 11, 12, 13]. This allows for event-by-event fluctuation analysis with high PID and tracking efficiencies, which amounts to about 80% for protons, almost independent of the collisions centrality. The latter is important because small efficiencies also reduce dynamical fluctuations of interest. As an input the method uses only the probabilities for each track in a given event of being a proton, kaon, pion or electron, which are calculated by exploiting fitting dE/dx distributions within the fine bins of track momentum and pseudorapidity [12, 13].

3. Results and discussions

In the left panel of Fig. 1 the centrality dependence of the second cumulants of net-protons, represented with the solid red boxes, is compared to the Skellam baseline depicted with the open boxes. We note that the Skellam baseline is calculated as the sum of the mean numbers (first cumulants) of protons (solid green circles) and antiprotons (open green circles) in the corresponding centrality class. Below we demonstrate the validity of this approach for the baseline calculation. As seen from the bottom panel of Fig. 1, deviations

of the second cumulants of net-protons from the Skellam baseline are observed for all centrality classes. In order to shed light on these observations we have reconstructed second cumulants of single proton and antiproton distributions which are depicted in in the left panel of Fig. 1 with the solid and open blue circles, respectively. We observe significant differences between second and first cumulants of single protons and anti-protons. The latter however does not necessarily indicate deviation of single proton and antiproton distributions from the underlying Poisson baseline. Indeed, within the recently proposed model it was demonstrated that dynamical fluctuations are significantly modified by the unavoidable fluctuations of participant nucleons [6] (see also Ref. [14]). The model uses several inputs such as mean number of protons and antiprotons and the centrality selection procedure which determines the fluctuations of participants. Using the experimentally measured mean values of protons and antiprotons presented in Fig. 1 and the same centrality selection as used in this analysis we calculated second cumulants of protons and net-protons in the presence of participant fluctuations. These results are presented with the dashed and solid lines in the left panel of Fig. 1 for protons and net-protons respectively. Both calculations are consistent with the experimentally measured second cumulants of protons and the Skellam distribution, correspondingly. We note that, in the model, particles are produced from the independent Poisson distributions, i.e, the difference between the dashed line and the mean values of protons is completely driven by the participant fluctuations. We therefore conclude that the observed deviation between the second and first cumulants of protons and antiprotons are stemming from participant fluctuations. On the other hand, the consistency between the solid line and the Skellam distribution shows that the second cumulants of net-protons at LHC energies are not affected by the participant fluctuations, which justifies the calculation of the Skellam baseline as a sum of the mean numbers of protons and antiprotons. According to Eq. 3 the only reason for the deviation of the experimentally measured second cumulants of net-protons from the corresponding second cumulants of the Skellam distribution can be due to the correlation term.

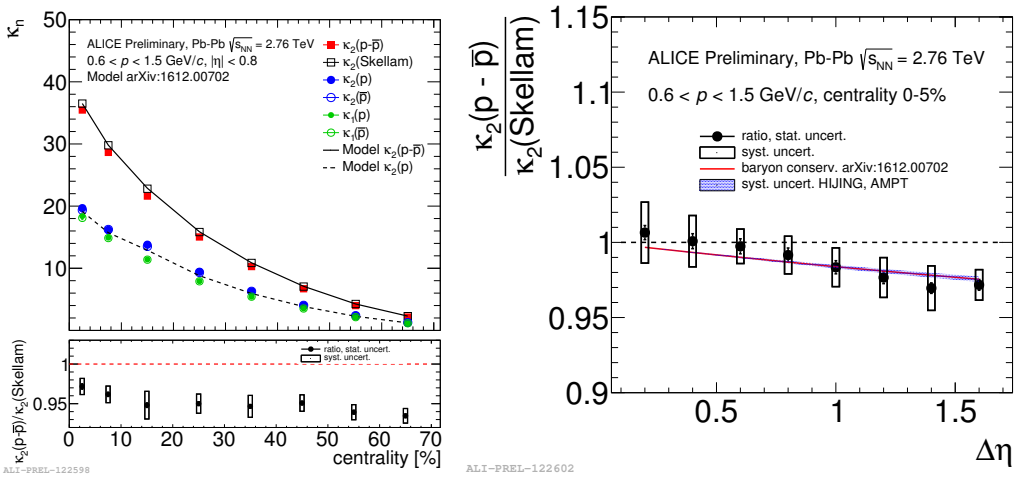

Fig. 1. Left panel: Experimentally measured second cumulants of net-proton distributions (red solid boxes) compared to Skellam baseline (open squares). The second cumulants of single proton and antiproton distributions are presented with the filled and open blue circles, correspondingly. The green solid and open circles represent first cumulants of protons and antiprotons respectively, which are hardly distinguishable because of the nearly equal mean numbers of protons and antiprotons. The model predictions with the underlying independent Poisson distributions for protons and antiprotons are depicted with the solid (net-protons) and dashed (protons) lines. In the bottom panel the ratio of the experimentally measured second cumulants of net-protons to the Skellam baseline is presented. Right panel: Pseudorapidity dependence of the normalised second cumulants of net-protons. The red solid line shows the effect of the baryon number conservation.

For the second cumulants the correlation term arising from the global baryon number conservation depends only on the acceptance factor $\alpha = \langle n_p \rangle / \langle N_B^{4\pi} \rangle$ with $\langle n_p \rangle$ and $\langle N_B^{4\pi} \rangle$ referring to the mean number of protons inside the acceptance and the mean number of baryons in the full phase space respectively [6]:

$$\frac{\kappa_2\,(p-\bar{p})}{\kappa_2\,(Skellam)} = 1-\alpha. \tag{4}$$

We performed our analysis in 8 different pseudo-rapidity ranges from $|\eta| < 0.1$ up to $|\eta| < 0.8$ in steps of 0.1. The obtained results for the second cumulants of net-protons, normalised to the Skellam baseline, are presented in the right panel of Fig. 1. For each rapidity range we estimated the acceptance factor α. In doing so, we used the total number of baryons as measured by the ALICE experiment in the pseudorapidity range of $|\eta| < 0.5$ [15]. Next, using HIJING and AMPT simulations, we obtained total number of baryons in the full phase space. The number of protons, used in the definition of α (cf. Eq. 4), is taken from the current analysis for each rapidity range. Finally, using these values of α the red band in Fig. 1 is calculated with Eq. 4. The finite width of the band reflects the difference between the two event generators.

As seen from the right panel of Fig. 1, for pseudorapidity ranges of $|\eta| < 0.4$, which corresponds to $\Delta\eta < 0.8$, the experimentally measured net-proton distributions follow a Skellam distribution. This agreement is due to the small acceptance as discussed above. Beyond $\Delta|\eta| > 0.8$ we do observe deviations from the Skellam distribution. The amount of deviation is in good agreement with the red band as calculated with Eq. 4. We hence conclude that this deviation is caused by global baryon number conservation and that other possible dynamical fluctuations are not visible in the second cumulants of net-protons.

4. Conclusions

In summary, we presented first measurements of net-proton fluctuations from the ALICE experiment at LHC. The measured second cumulants of net-protons, which are used as a proxy for net-baryons, are, after accounting for baryon number conservation, in agreement with the corresponding second cumulants of the Skellam distribution. We note that LQCD predicts a Skellam behaviour for the second cumulants of net-baryon distributions at a pseudo-critical temperature of about 155 MeV, which is very close to the freeze-out temperature from the HRG model applied to the ALICE data [4, 16]. Critical behaviour is predicted by LQCD for higher cumulants of net-baryon distributions, which will be the topic of our further investigations [16].

Acknowledgments

This work is part of and supported by the DFG Collaborative Research Centre "SFB 1225 (ISOQUANT)".

References

[1] A. Bazavov et al., Phys. Rev. D85 (2012) 054503.
[2] B. Friman, F. Karsch, K. Redlich, and V. Skokov, Eur. Phys. J. C71 (2011) 1964.
[3] L. D. Landau and E. M. Lifshitz, Statistical Physics, Pergamon Press, 1980.
[4] A. Andronic, P. Braun-Munzinger, K. Redlich, and J. Stachel, proceedings of SQM 2016, arXiv:1611.01347.
[5] V. Koch, in "Relativistic Heavy Ion Physics", R. Stock (ed.) (Springer, Heidelberg, 2010), (Landolt-Boernstein New Series I, v. 23) p. 626, arXiv:0810.2520v1.
[6] P. Braun-Munzinger, A. Rustamov, J. Stachel, Nucl. Phys. A960 (2017), 114.
[7] M. Kitazawa, and M. Asakawa, Phys. Rev. C86 (2012) 024904 and erratum, ibidum 069902, arXiv:1205.3292 [nucl-th].
[8] K.Aamodt et al. (ALICECollab.), JINST3, (2008) S08002.
[9] M. Gazdzicki et al., Phys. Rev. C83 (2011) 054907 .
[10] M. I. Gorenstein, Phys. Rev. C84 (2011) 024902.
[11] A. Rustamov, M. I. Gorenstein, Phys. Rev. C86 (2012) 044906.
[12] T. Anticic et al. (NA49 Collab.), Phys.Rev. C89 (2014) 054902.
[13] M. Arslandok (ALICE Collab.), Nucl.Phys. A956 (2016) 870-873.
[14] V. Skokov, B. Friman, and K. Redlich, Phys.Rev. C88 (2013) 034911.
[15] P. Braun-Munzinger, A. Kalweit, K. Redlich, and J. Stachel, Phys.Lett. B747 (2015) 292.
[16] F. Karsch, these proceedings.